

ORIGINAL ARTICLE

Open Access



Effects of Redispersible Polymer Powder on Mechanical and Durability Properties of Preplaced Aggregate Concrete with Recycled Railway Ballast

Sahyeon Lee¹, Seung Yup Jang², Chan Young Kim¹, Eun Jong Ahn¹, Seung Pil Kim¹, Seongwoo Gwon¹ and Myoungsu Shin^{1*}

Abstract

The rapid-hardening method employing the injection of calcium sulfoaluminate (CSA) cement mortar into voids between preplaced ballast aggregates has recently emerged as a promising approach for the renovation of existing ballasted railway tracks to concrete tracks. This method typically involves the use of a redispersible polymer powder to enhance the durability of the resulting recycled aggregate concrete. However, the effects of the amount of polymer on the mechanical and durability properties of recycled ballast aggregate concrete were not clearly understood. In addition, the effects of the cleanness condition of ballast aggregates were never examined. This study aimed at investigating these two aspects through compression and flexure tests, shrinkage tests, freezing–thawing resistance tests, and optical microscopy. The results revealed that an increase in the amount of polymer generally decreased the compressive strength at the curing age of 28 days. However, the use of a higher polymer ratio enhanced the modulus of rupture, freezing–thawing resistance, and shrinkage resistance, likely because it improved the microstructure of the interfacial transition zones between recycled ballast aggregates and injected mortar. In addition, a higher cleanness level of ballast aggregates generally improved the mechanical and durability qualities of concrete.

Keywords: railway ballast, concrete track, calcium sulfoaluminate (CSA) cement, redispersible polymer powder, preplaced aggregate concrete, interfacial transition zone (ITZ)

1 Background

In modern times, the enhancement of the traveling speed and capacity of trains have been among the main issues facing public transportation systems around the world. These needs have been met by the continuous advancement of the classical railway track system, which consists of ballasted tracks, along with the development of train technologies (Bezin et al. 2010).

Despite many modifications over its history, the ballasted track system continues to present considerable problems, such as changes in the track geometry, fast deteriorations of track components, and rising maintenance and repair costs due to increasing train speed and transport capacity (Miura et al. 1998; Bezin et al. 2010). Accordingly, the need for non-ballasted railway tracks with higher durability has gradually increased worldwide (Galvín et al. 2010; Lee et al. 2016). For example, the percentage of slab tracks for Japanese high-speed lines has greatly increased since the introduction of the Sanyo Shinkansen line in 1972 (Miura et al. 1998; Paixão et al. 2009). The use of slab tracks has also risen in many European countries (Paixão et al. 2009).

Recently, an effective method for upgrading existing ballasted tracks to non-ballasted tracks has been

*Correspondence: msshin@unist.ac.kr

¹ School of Urban and Environmental Engineering, Ulsan National Institute of Science and Technology (UNIST), 50 UNIST-gil, Ulsan 44919, Republic of Korea

Full list of author information is available at the end of the article
Journal information: ISSN 1976-0485 / eISSN 2234-1315

developed in Japan (Higuchi et al. 1978) and South Korea (Lee et al. 2016). This method, so-called the rapid-hardening method, is used to transform a ballasted track into a concrete track by injecting calcium sulfoaluminate (CSA) cement mortar into voids between preplaced ballast aggregates and solidifying the whole composite as preplaced aggregate concrete (PAC), as illustrated in Figs. 1 and 2 (Murao and Aihara 2005; Jang et al. 2013). This method may take less than 5 h to produce a concrete track with a sufficient strength, so that it may not require any interruption of train operations. In South Korea, an early version of the rapid-hardening method was applied to some urban railway lines (Jang et al. 2013), and a more advanced method and materials for use in high-speed railway lines are being developed by our research group (Korean Railroad Research Institute 2014).

Coarse aggregates in existing ballasted tracks typically have fine particles and pollutants attached to their surfaces. Such alien materials are likely to impact on the properties of the resulting concrete by weakening the interfacial transition zones (ITZs) between the aggregates and mortar (Muñoz et al. 2005; Norvell et al. 2007; McNeil and Kang 2013; Kim et al. 2013; Kang et al. 2014; Choi et al. 2016a). Furthermore, the strength and durability of PAC are more greatly influenced by the properties of coarse aggregates than those of cast-in-place concrete, because of their higher volumetric ratio in PAC (ACI Committee 304 2000; Najjar et al. 2014). Indeed, previous studies reported that PAC produced from recycled ballast aggregates showed inferior freezing–thawing resistance due to interfacial failures between the aggregates and mortar as shown in Fig. 3 (Korean Railroad Research

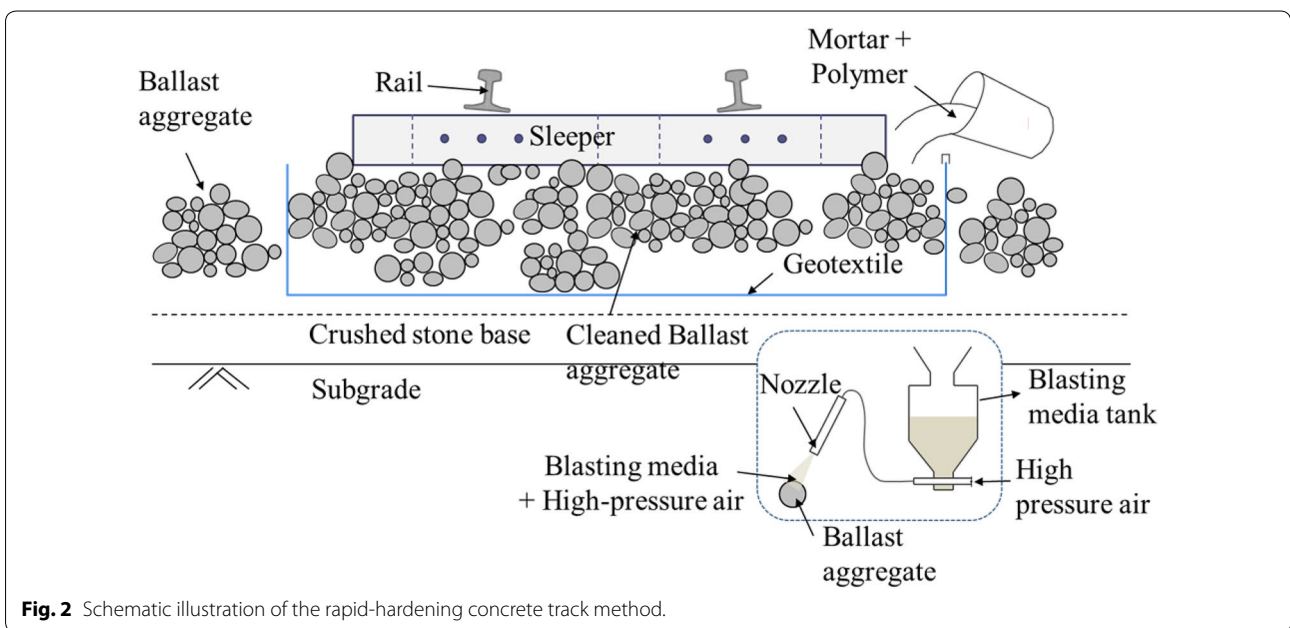
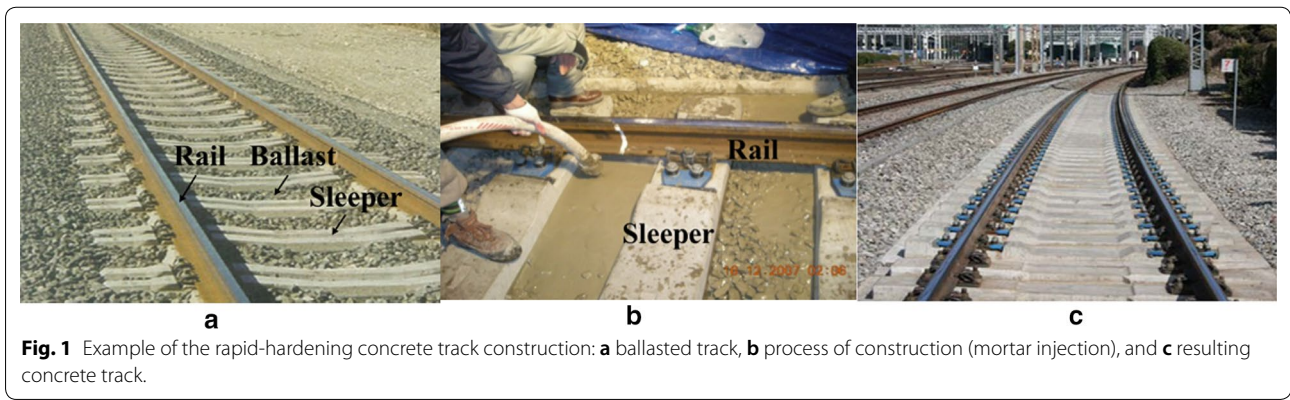
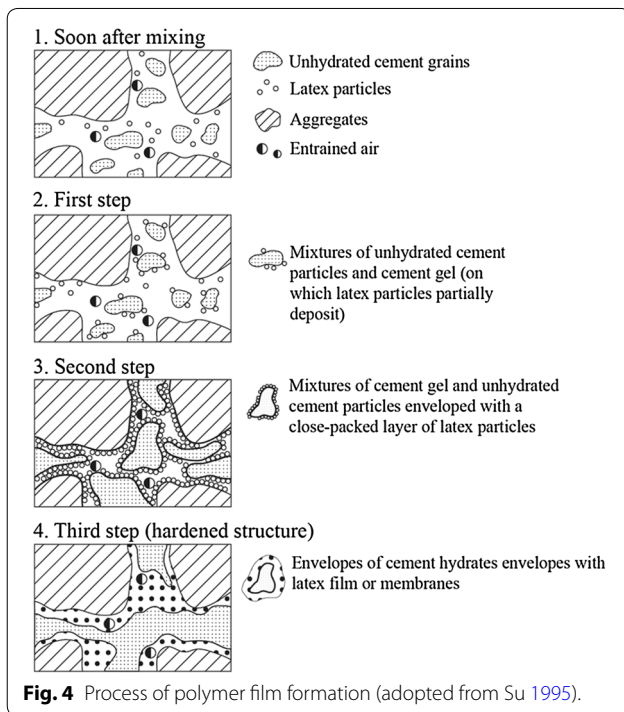




Fig. 3 Interfacial failure between recycled ballast aggregates and mortar in freezing–thawing tests (Yoo et al. 2016).



Institute 2015; Yoo et al. 2016). Therefore, the quality of the ITZs between ballast aggregates and mortar is considered a critical factor for the strength and durability of the PAC resulting from the rapid-hardening method.

Several researchers attempted to use a polymer to enhance the microstructure of ITZs in concrete (Ohama 1995; Su 1995; Kardon 1997; Kim and Robertson 1998). Some studies suggested that the polymer formed continuous films or membranes in the microstructure of concrete (Ohama 1995; Su 1995). They proposed that the polymer films bound cement hydrates to one another and to aggregates, and filled pores in the concrete, as shown in Fig. 4 (Su 1995). Thus, the polymer helped to create a denser microstructure by reducing the volume of porous transition zones and to strengthen the binding of aggregates to the cement-based matrix (Shaker et al. 1997; Choi et al. 2016b; Liu et al. 2018; Qudoos et al. 2018).

This was considered capable of improving the durability of concrete as a consequence (Ohama 1995; Su 1995; Kardon 1997; Shaker et al. 1997; Rossignolo and Agnesini 2004; Aggarwal et al. 2007). However, the properties of concrete are likely influenced by the type and amount of polymer (Ohama 1995), which has not been fully understood to date.

Another way of improving the microstructure of ITZs in the resulting concrete would be to remove pollutants from the surfaces of ballast aggregates. However, the cleaning process requires additional time and cost, and it produces environmental pollutants such as dust and noise (Lee 2010). Hence, the effects of different cleanness levels of ballast aggregates need to be examined to minimize the construction time and cost while meeting the strength and durability requirements of concrete.

Given the aforementioned concerns, the effects of the amount of polymer and the cleanness level of aggregates on the mechanical and durability properties of PAC produced from recycled ballast aggregates were investigated in this study. Compression and flexure tests, shrinkage tests, freezing–thawing resistance tests, and optical microscopy were conducted by varying the amount of a dispersible polymer powder and the cleanness level of ballast aggregates.

2 Materials and Specimens

2.1 Materials

The cement used is calcium sulfoaluminate (CSA) cement containing a higher portion of aluminum oxide than Portland cement, as indicated by the chemical oxide composition in Table 1. The Blaine fineness and LOI (loss on ignition) of the cement are 4800 cm²/g and 1.6% respectively. The polymer used is acrylic redispersible polymer powder (Fig. 5a), and its chemical oxide composition and other properties are summarized in Table 2. The particle size distribution of the polymer powder is plotted in Fig. 6. Two different set retarders were used: citric acid and zinc acetate. Citric acid functions as both a set retarder and water reducer, and zinc acetate functions as a set retarder. The set retarders were used to ensure a

Table 1 Chemical oxide composition of cement.

Chemical oxide composition (%)							
CaO	SO ₃	SiO ₂	Al ₂ O ₃	MgO	Fe ₂ O ₃	Others	
54.6	14.6	12.4	11.8	2.34	2.25	2.05	

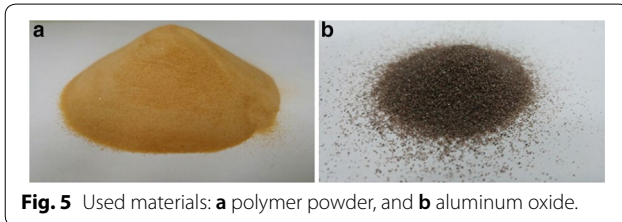


Fig. 5 Used materials: **a** polymer powder, and **b** aluminum oxide.

Table 2 Chemical oxide composition and other properties of polymer.

Chemical oxide composition (%)				Other properties
SO ₃	SiO ₂	CaO	Others	Bulk density (kg/m ³)
45.9	26.2	24.9	3.07	540

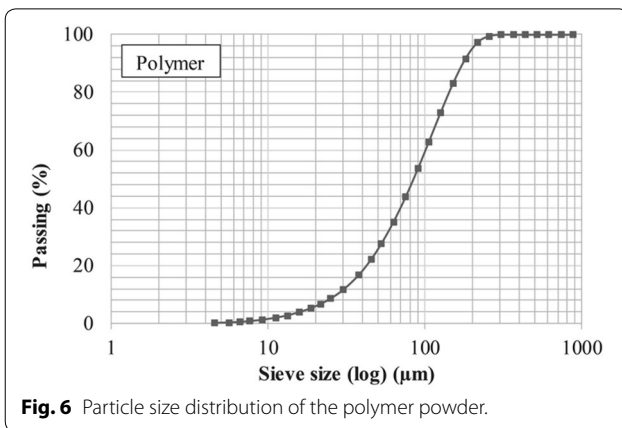


Fig. 6 Particle size distribution of the polymer powder.

sufficient workable time because the CSA cement starts to harden quickly right after water is mixed.

The ballast aggregates used in this study were acquired from a real ballasted railway track. The recycled ballast aggregates were prepared at three different levels of surface cleanliness (i.e., H-, M-, or L-level) as shown in Fig. 7. H-level aggregates represented the highest level of cleanliness among the three categories; they were dry-cleaned using a blasting method (Lee et al. 2015) until all visible dusty particles attached to the surface were removed (for about 3 min at 0.5 MPa). The blasting method used aluminum oxide (Al₂O₃) as a general high-pressured blasting

agent (Fig. 5b) to peel off the attached particles. M-level aggregates represented the medium level of cleanliness among the three categories; they were dry-cleaned by the blasting method for 30 s. In contrast, L-level aggregates represented the lowest level of cleanliness; no cleaning treatment was applied to them.

The physical and chemical properties of the ballast aggregates with three different cleanliness levels are presented in Table 3. For the H-, M-, and L-level aggregates, the fine materials passing through a 0.08-mm sieve are 0.1, 0.06, and 0.04%, respectively, and the abrasion test results are 6.7, 6.5, and 6.4%, respectively. The qualities of the recycled ballast aggregates were considerably higher than the standard requirements for recycled coarse aggregate in KS F 2573 (Kim et al. 2013).

The particle size distributions of fine and ballast aggregates are plotted in Fig. 8. Because the maximum size of ballast aggregates was slightly larger than 60 mm (Fig. 7), only ballast aggregates passing through a 40-mm sieve were used for the concrete tests of this study, as specified in KS F 2403 (Korean Standards Association 2014a, b). Note that ASTM C192 (2016) specifies that the sample should be created by wet sieving through a 50-mm sieve when the maximum size of coarse aggregate is larger than 50 mm. In this study, however, a 40-mm sieve was used, considering that the freeze–thaw tests were conducted on 100 × 100 × 400 mm specimens according to ASTM C666 (2016).

2.2 Test Variables and Mix Proportions

In this study, the main test variables were the amount of polymer and the cleanliness level of recycled ballast aggregates. The polymer ratio was varied as 0, 2, 6, and 10% of the total weight of cement. The cleanliness level of ballast aggregates was classified as one of the three categories (H-, M-, or L-level) according to the amount of alien particles remaining on the aggregate surface, as described in the previous section.

Table 4 summarizes the proportions of a total of sixteen different mix cases; four mortar samples and twelve concrete samples were tested. The W/C ratio, in which W and C signify water and cement, respectively, was fixed at 39.3% in all sixteen mix cases. The contents of the retarders A and B, which are citric acid and zinc acetate respectively, were fixed at 0.16% and 0.12% of the weight of cement, respectively.

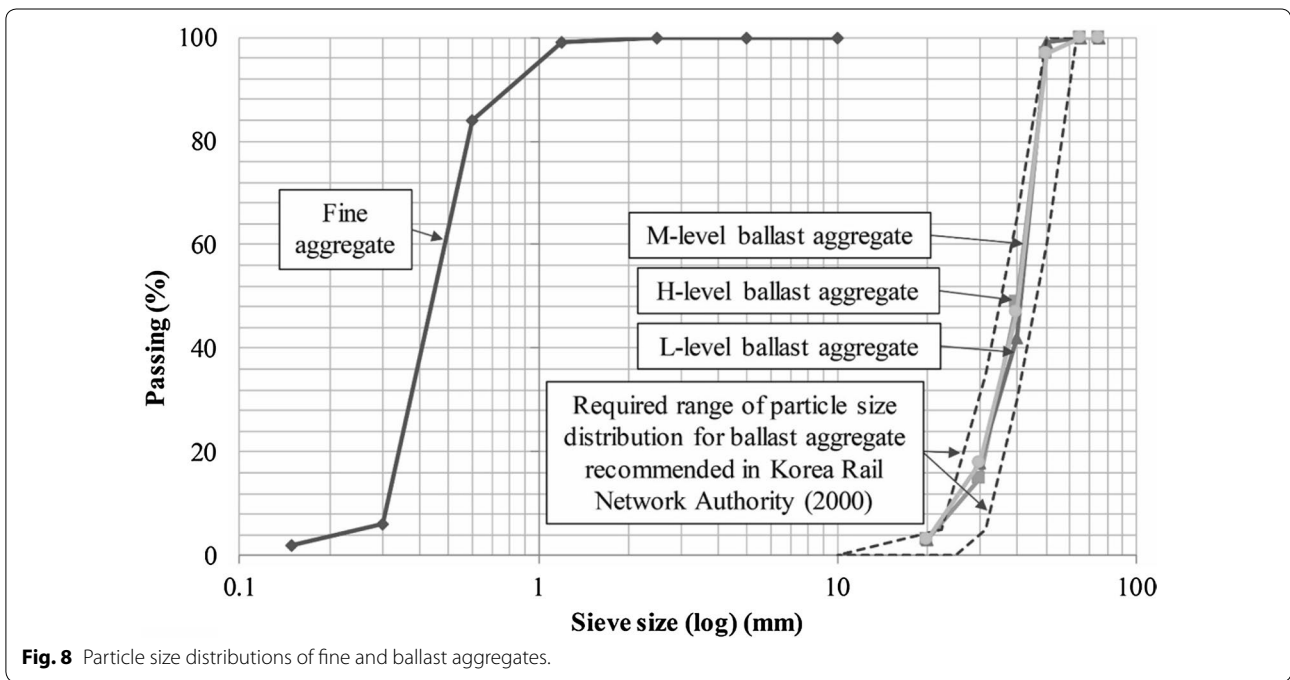


Table 3 Physical and chemical properties of fine and ballast aggregates.

Property	Fine aggregate	Ballast aggregates		
		L-level	M-level	H-level
Absorption (%)	1.53	0.52	0.47	0.48
Abrasion (%)	–	6.7	6.5	6.4
0.08 mm sieve passing (%)	2.2	0.1	0.06	0.04
Alkali aggregate reaction	–	Harmless	Harmless	Harmless
Stability (%)	2.4	3.1	1.9	2.0
Absolute dry density (g/cm ³)	2.55	2.60	2.60	2.61

Table 4 Mix proportions of four mortar samples and twelve concrete samples.

Group	Sample	W/C	Unit weight (kg/m ³)						
			W	C	Fine aggregate	Ballast aggregate	Polymer	Retarder	
								A	B
Mortar	C-0	39.3%	339	862	923	–	0	1.43	1.07
	C-2		339	862	923	–	17.9	1.43	1.07
	C-6		339	862	923	–	53.6	1.43	1.07
	C-10		339	862	923	–	89.3	1.43	1.07
Concrete	C-H-0		186	473	507	1446	0	0.78	0.59
	C-H-2		186	473	507	1446	9.80	0.78	0.59
	C-H-6		186	473	507	1446	29.4	0.78	0.59
	C-H-10		186	473	507	1446	49.0	0.78	0.59
	C-M-0		186	473	507	1446	0	0.78	0.59
	C-M-2		186	473	507	1446	9.80	0.78	0.59
	C-M-6		186	473	507	1446	29.4	0.78	0.59
	C-M-10		186	473	507	1446	49.0	0.78	0.59
	C-L-0		186	473	507	1446	0	0.78	0.59
	C-L-2		186	473	507	1446	9.80	0.78	0.59
	C-L-6		186	473	507	1446	29.4	0.78	0.59
	C-L-10		186	473	507	1446	49.0	0.78	0.59

2.3 Mixing, Casting, and Curing Procedures

The procedure according to which PAC specimens were prepared is shown in Fig. 9. Firstly, specimen molds were filled with ballast aggregates, and were shaken on a vibrating table to pack the aggregates densely. Next, mortar (a mixture of cement and fine aggregate) and polymer were dry-mixed by a mechanical mixer. Then, the dry-mixed mortar and polymer were poured into the water in which the retarders were dissolved. Then, all materials were blended together at a paddle speed of about 100 rpm. Lastly, the fresh plastic mortar was inserted into the specimen molds as the sides of the molds were lightly tapped with a rubber mallet to ensure even distribution of the plastic mortar in the voids between ballast aggregates and to remove air from inside the mortar. For mortar samples with no ballast aggregates, the first step (packing aggregates into specimen molds) was omitted.

For shrinkage tests, one strain gauge and one thermocouple were embedded within each specimen to measure the specimen shrinkage and temperature (Fig. 10). First, the mold was filled with ballast aggregates up to mid-height and was subjected to vibration on a vibrating table. On the placed ballast aggregates, a strain gauge (EGP-5-120, with a gauge length of 100 mm and outer body size of 130 × 17 × 10 mm) and a thermocouple were installed in the longitudinal direction of the mold as shown in Fig. 10. Next, the top half of the mold was carefully filled with ballast aggregates, and the mold was vibrated again to pack the aggregates densely. Finally, fresh mortar was inserted into the mold while tapping the sides of the mold lightly with a rubber mallet.

After the molds were removed, the hardened specimens were dry-cured in an air-conditioned room at a temperature of 20 ± 3 °C and relative humidity of 60% until the tests were conducted.



Fig. 9 Procedure for the fabrication of tested PAC specimens: **a** sieving, **b** packing aggregates in a mold, **c** mixing mortar, **d** filling the mold with mortar, and **e** curing.

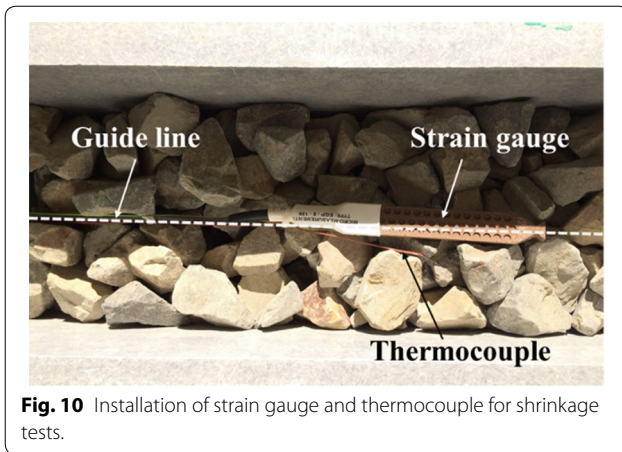


Fig. 10 Installation of strain gauge and thermocouple for shrinkage tests.

3 Test Methods

3.1 Compression Test

Compression tests for mortar samples with no ballast aggregates (Table 4) were carried out on 50-mm long cube specimens according to ASTM C109 (2016). For concrete samples containing ballast aggregates (Table 4), cylindrical specimens 150 mm in diameter and 300 mm in height were used according to ASTM C39 (2016). The compression tests were conducted at 28 days of curing, as well as at the early hours of curing noted in Table 5,

and three specimens were tested for each case. In particular, the compression tests at the early hours of curing were conducted to investigate the effect of the polymer on the early strength development. For the cylindrical specimens, three LVDTs were installed to estimate the axial strain, as shown in Fig. 11a.

3.2 Flexure Test

The effects of the test variables on the tensile capacity of PAC with recycled ballast aggregates were investigated by modulus-of-rupture tests in accordance with ASTM C78 (2016). The flexure tests were conducted using third-point loading on prism specimens with the dimensions of 150 × 150 × 550 mm. For each concrete sample in Table 4, three specimens were tested after 28 days of curing. The vertical displacement of a specimen was measured by installing two LVDTs at the midspan of the specimen as shown in Fig. 11b, and the average of the two values was used as the deflection of the specimen.

3.3 Shrinkage Test

For each concrete sample in Table 4, shrinkage tests were conducted on three prism specimens with a size of 150 × 150 × 550 mm. The shrinkage test specimens were cured in an air-conditioned room under controlled temperature of 20 ± 3 °C and relative humidity of 60% during the entire test period. The embedded strain gauge and

Table 5 Compressive strength and modulus of elasticity.

Sample	Compressive strength (MPa)								Modulus of elasticity (GPa)	
	Curing time								ACI Committee 318 (2014)	ASTM C469 (2014)
	2 h		3 h		4 h		28 days			
Average	St. dev.	Average	St. dev.	Average	St. dev.	Average	St. dev.			
C-0	23.5	0.86	–	–	–	–	59.8	3.40	–	–
C-2	25.8	1.63	–	–	–	–	56.6	2.81	–	–
C-6	17.1	1.07	–	–	–	–	54.9	1.18	–	–
C-10	10.3	0.13	–	–	–	–	45.4	0.75	–	–
C-H-0	13.8	0.68	–	–	–	–	38.7	2.76	29.4	73.6
C-H-2	9.91	0.77	–	–	–	–	35.3	2.34	28.1	27.0
C-H-6	–	–	9.49	0.86	–	–	32.4	0.65	26.9	25.0
C-H-10	–	–	–	–	11.1	2.10	29.8	2.44	25.8	31.8
C-M-0	12.7	2.61	–	–	–	–	33.0	6.70	27.1	66.1
C-M-2	8.63	2.74	–	–	–	–	23.0	1.59	22.7	20.3
C-M-6	–	–	7.28	1.59	–	–	20.1	1.32	21.2	27.2
C-M-10	–	–	–	–	8.01	0.82	25.3	1.57	23.8	90.8
C-L-0	8.27	1.62	–	–	–	–	32.6	3.45	27.0	57.0
C-L-2	9.86	1.51	–	–	–	–	34.3	1.58	27.7	27.0
C-L-6	–	–	6.84	1.09	–	–	33.6	2.13	27.4	26.5
C-L-10	–	–	–	–	5.94	0.39	22.0	2.61	22.1	45.1

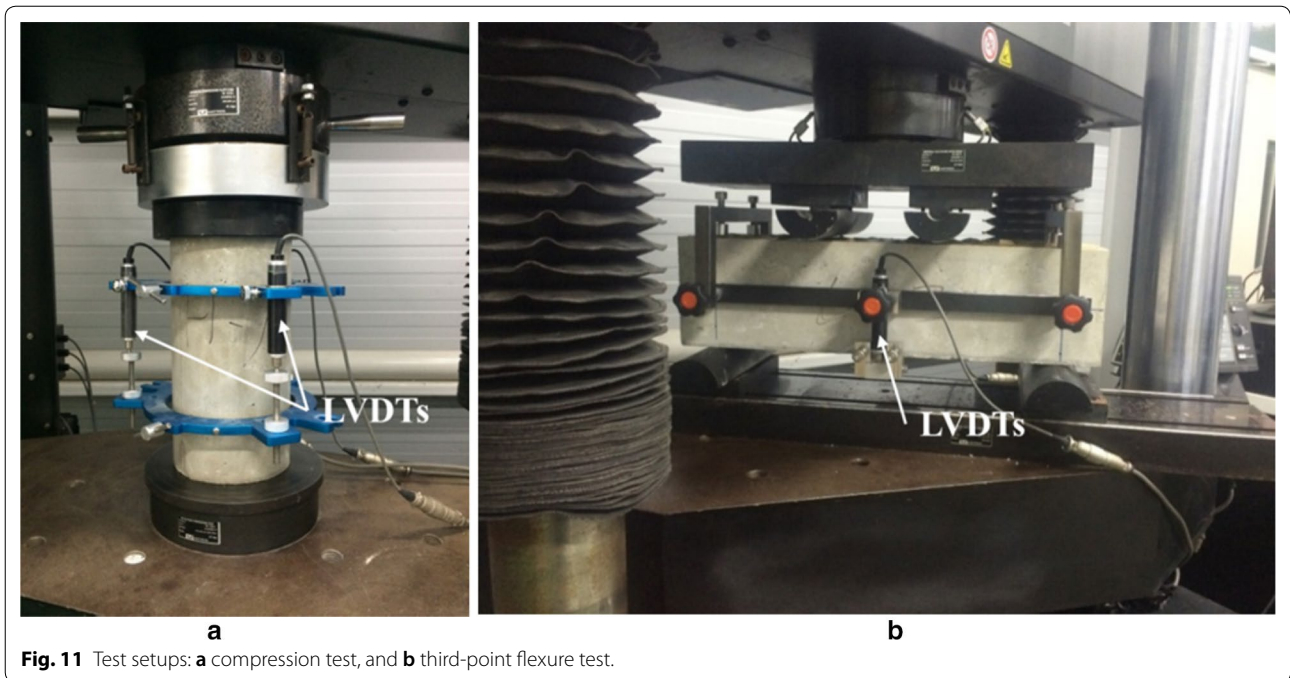


Fig. 11 Test setups: **a** compression test, and **b** third-point flexure test.

thermocouple (Fig. 10) were connected to a data logger (TDS-530) after 3 h of curing, and the change in length and temperature of each specimen were measured and recorded for 91 days. After the tests, the effect of temperature on the shrinkage strain was compensated for, based on the measured temperature data of the specimen (Yang and Joo 2011).

3.4 Freezing–Thawing Resistance Test

Freezing–thawing resistance tests were performed for concrete samples by using prism specimens with a size of 100 × 100 × 400 mm according to ASTM C666 (2016); three specimens were tested for each sample. The initial fundamental transverse frequency and mass of each specimen were measured at 14 days of curing under a controlled temperature of 20 ± 3 °C and relative humidity of 60%. Then, the specimens were placed in the test apparatus filled with water, and were subjected to temperature cycles between − 18 °C and 4 °C, which were controlled by monitoring the interior temperature of a control specimen, as shown in Fig. 12.

At about 36 cycle intervals, the fundamental transverse frequency and mass were measured, and the relative dynamic modulus of elasticity (RDM) was calculated by:

$$P_c = \left(\frac{n_c^2}{n_0^2} \right) \times 100 \tag{1}$$



Fig. 12 Test setup: freezing–thawing resistance test.

Here, P_c is the relative dynamic modulus of elasticity (%), n_c is the fundamental transverse frequency after c cycles, and n_0 is the fundamental transverse frequency at the beginning of the test (at 14 days of curing). The test was discontinued when P_c was reduced to below 60% of the initial modulus or after 300 cycles, whichever occurred first.

Based on the freezing–thawing test results, the durability factor of concrete was calculated by:

$$DF = P_N(N/300) \tag{2}$$

Here, DF is the durability factor of the test specimen, P_N is the relative dynamic modulus of elasticity after N cycles (%), N is the number of cycles at which P_N reaches the specified minimum value for discontinuing the test (i.e., 60%) or the specified number of cycles at which the exposure is to be terminated (i.e., 300), whichever is less. After the tests, all the specimens were cut at a transverse section, and the ITZs between ballast aggregates and mortar in the cut section were observed by using an optical microscope.

4 Test Results

4.1 Compressive Strength and Modulus of Elasticity

The test results of compressive strength and elastic modulus for all mortar and concrete samples are summarized in Table 5; at least three specimens were tested for each sample.

The compressive strength tests at 2, 3 or 4 h of curing were conducted right after the surfaces of the specimens

solidified. The initial setting time was delayed as the amount of polymer increased under the condition that the same W/C ratio and retarders were used in all mix samples. Thus, the specimens containing 0% or 2% polymer were tested at about 2 h of curing, the specimens with 6% polymer were tested at about 3 h of curing, and the specimens with 10% polymer were tested at about 4 h of curing. This delay in the setting time was likely attributed to the films the polymer particles produced around cement grains, as these films would inhibit the reaction between cement and water (i.e., cement hydration) (Su 1995; Wang et al. 2006, 2016).

The compressive stress–strain relationships of all twelve concrete samples (Table 4) acquired at 28 days of curing are presented in Figs. 13, 14 and 15. Note that there are only two plots in Fig. 15a, since one specimen of the sample (C-L-0) improperly failed during the test. The compressive strengths of all mortar and concrete samples at 28 days of curing are compared in Fig. 16. For a given polymer ratio, the mortar samples had a 50–175% higher compressive strength on average than the concrete samples. This implies that the compressive strength of PAC with recycled ballast aggregates was greatly affected by

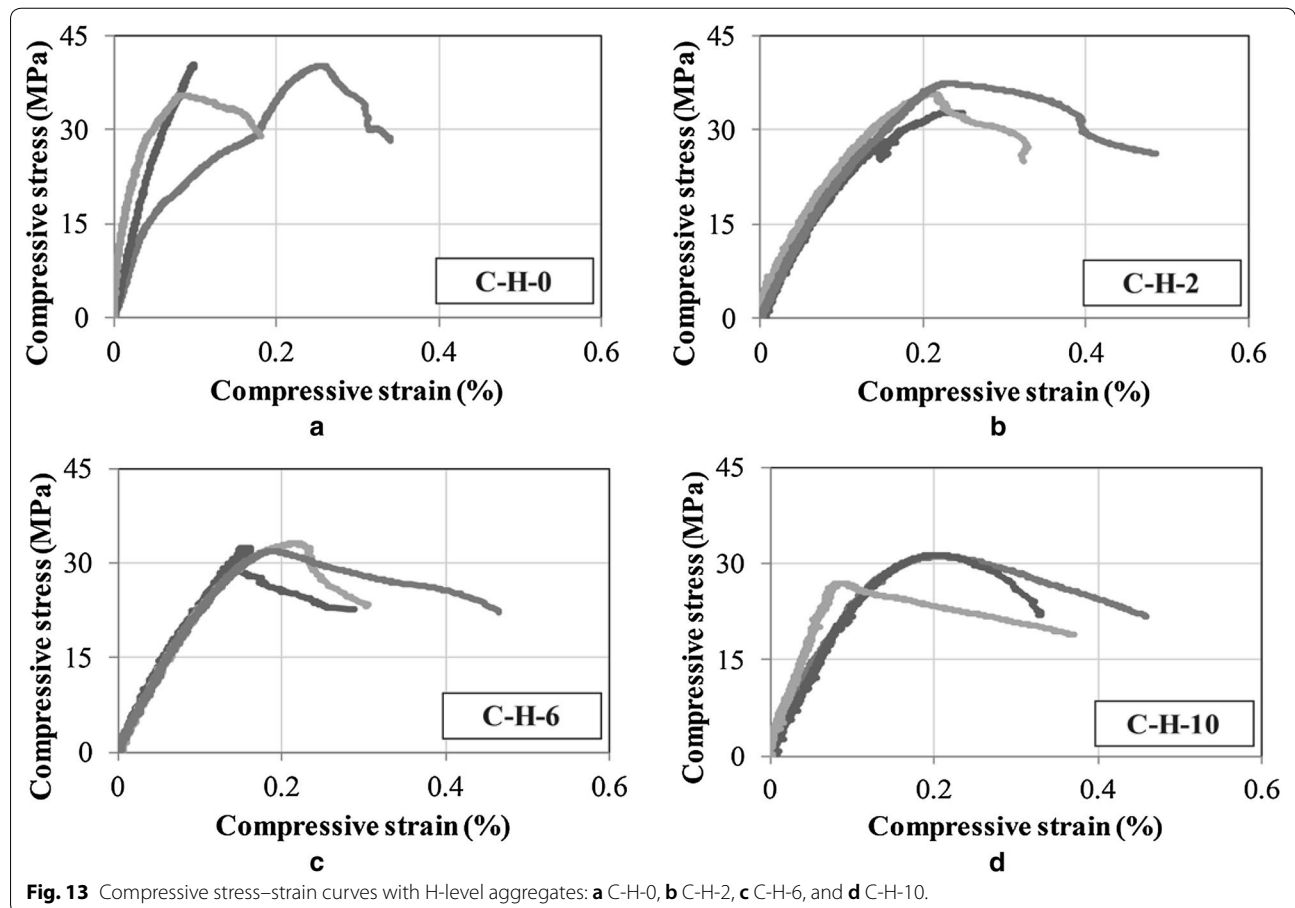
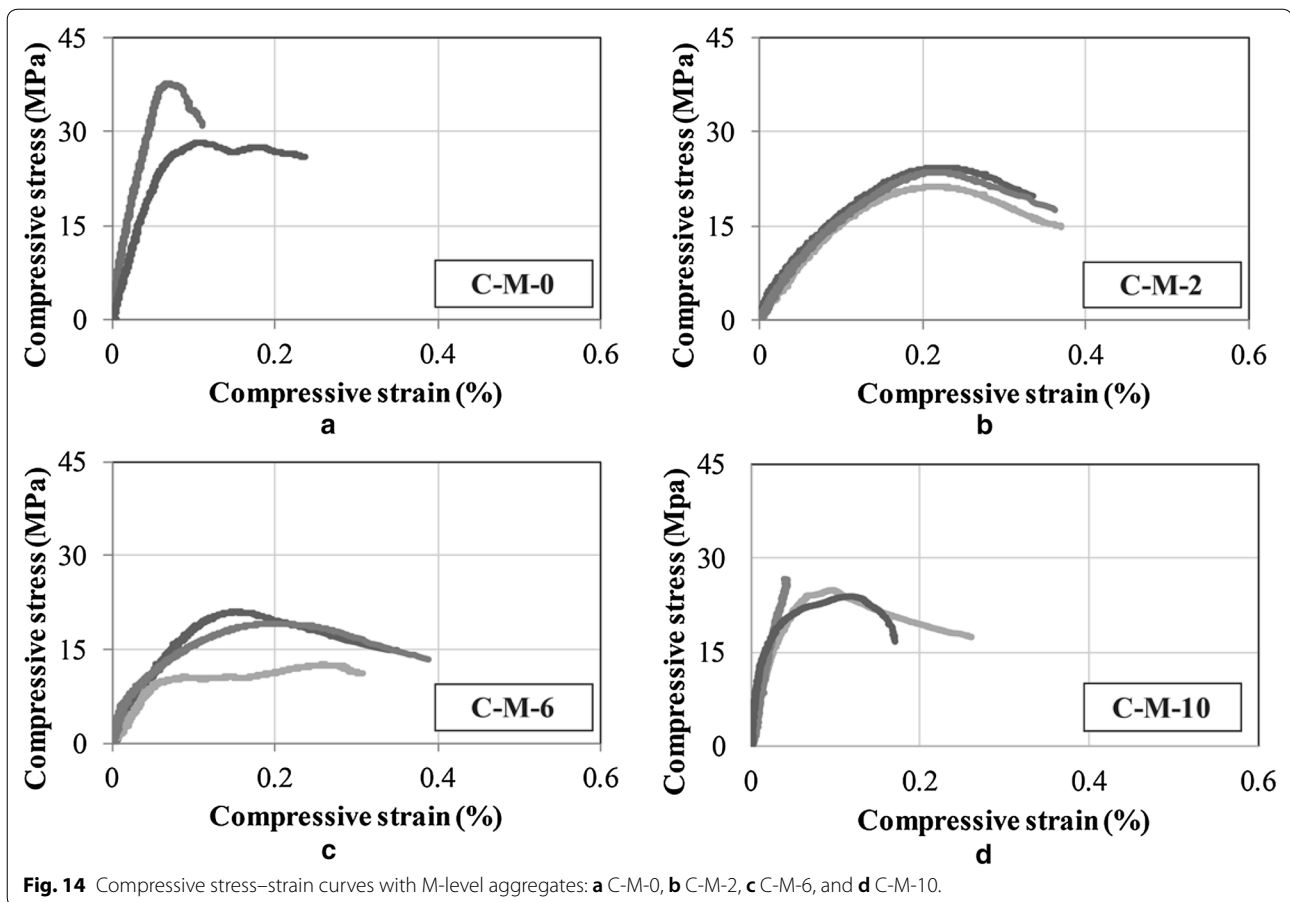


Fig. 13 Compressive stress–strain curves with H-level aggregates: **a** C-H-0, **b** C-H-2, **c** C-H-6, and **d** C-H-10.

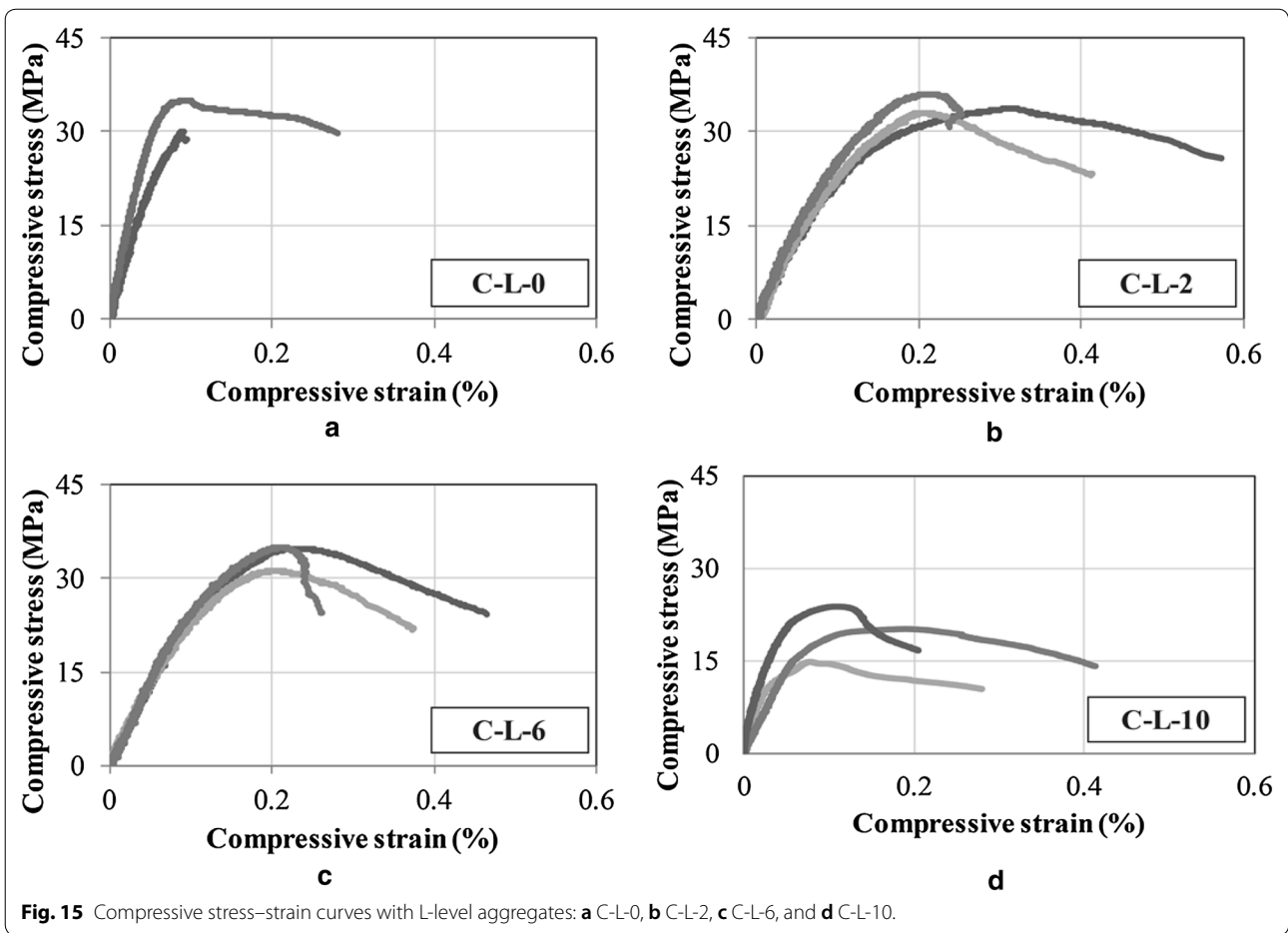


the ITZs between the mortar and aggregates (Najjar et al. 2014).

In both mortar and concrete cases, the compressive strength generally decreased as the polymer ratio increased (Fig. 16). With regard to the mortar samples, C-2, C-6, and C-10 had approximately 5.4, 8.2, and 24% lower compressive strengths than C-0, respectively. The reduction in strength was moderate up to a polymer ratio of 6%, but it was substantial at a ratio of 10%. For the concrete samples with H-level aggregates, C-H-2, C-H-6, and C-H-10 showed a compressive strength approximately 8.8, 16, and 23% lower than C-H-0. With a similar trend, C-M-10 and C-L-10 presented compressive strengths approximately 23 and 33% lower than C-M-0 and C-L-0, respectively. A lower compressive strength from a higher polymer ratio was likely attributed to the following: (1) the polymer particles hindered the cement from reacting with water, so that the strength development was delayed (Su et al. 1991; Su 1995; Jun et al. 2003). (2) Due to the low strength of the polymer itself, the polymer films had a similar effect to pores in the hardened concrete (Sakai and Sugita 1995).

Figure 17 plots the moduli of elasticity of all concrete samples, determined by ACI Committee 318 (2014) (see Table 5). The modulus of elasticity presented a tendency to decrease with increasing polymer ratio; the moduli of C-H-2, C-H-6, and C-H-10 were roughly 4.4, 8.5, and 12.2% smaller than that of C-H-0. Similarly, the moduli of C-M-10 and C-L-10 were 12.5 and 32.5% smaller than those of C-M-0 and C-L-0, respectively. This suggests that an increase in the polymer ratio generally caused a reduction in both the compressive strength and elastic modulus of PAC made from recycled ballast aggregates.

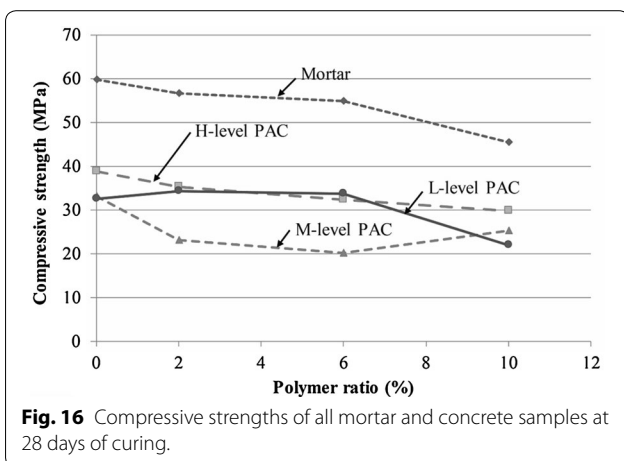
Regarding the cleanness level of ballast aggregates, the specimens with H-level aggregates generally showed higher compressive strengths than those with L- and M-level aggregates for a given polymer ratio (Fig. 16). The trend of a higher strength with H-level aggregates was particularly distinct at 10% polymer ratio; the compressive strength of C-H-10 was roughly 18% and 26% higher than those of C-M-10 and C-L-10, respectively. A possible reason for this result is that denser ITZs between the mortar and aggregates were created using H-level aggregates with smaller amounts of dusty particles. However,



the effect of the aggregate cleanness level was not apparent for polymer ratios of 2 and 6%.

4.2 Modulus of Rupture

Figure 18 compares the moduli of rupture (i.e., tensile strengths) of all concrete samples listed in Table 4. With



regard to the effect of the polymer, the specimens with a polymer ratio of 10% generally displayed the largest tensile strengths; the moduli of rupture of C-H-10 and C-L-10 were about 13.1 and 5.4% larger than those of C-H-0 and C-L-0, respectively.

In addition, the tensile-to-compressive strength (M/C) ratios are presented in Fig. 16; the ratios ranged from approximately 0.75–0.14. Although the samples containing 2 and 6% polymer had slightly smaller moduli of rupture than those containing no polymer, their M/C ratios were similar to or larger than those with no polymer. Furthermore, the M/C ratio increased sharply at 10% polymer ratio (except for M-level aggregate concrete). Therefore, it can be concluded that the use of polymer enhanced the ITZs between the ballast aggregates and mortar, and consequently improved the tensile strength.

As regards the effect of the cleanness level of ballast aggregates, the concrete samples of H-level aggregates showed higher tensile strengths than those of M- or L-level aggregates (Fig. 18). The modulus of rupture of C-H-10 was 24.3 and 11.3% higher than that of C-M-10 and C-L-10, respectively. However, the M-level aggregate

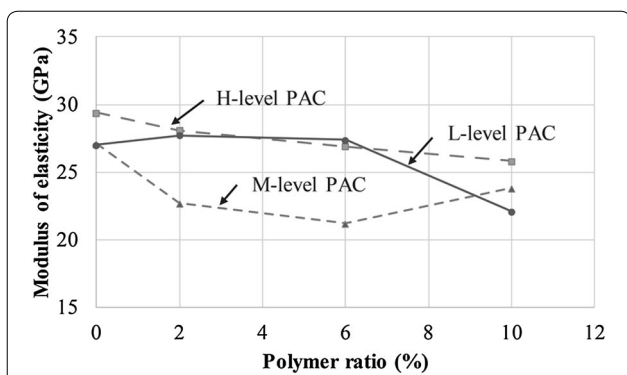


Fig. 17 Moduli of elasticity of all concrete samples at 28 days of curing.

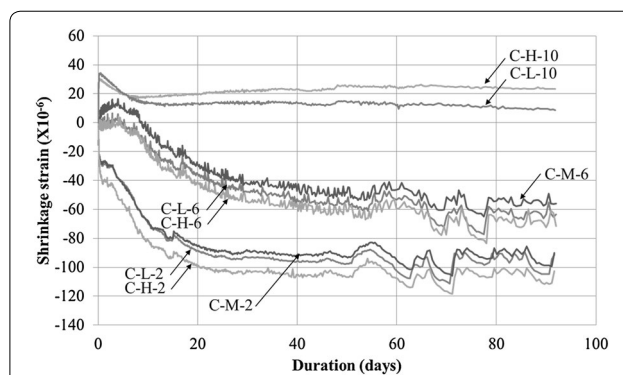


Fig. 19 Shrinkage strains of concrete samples with 2, 6, or 10% polymer ratio.

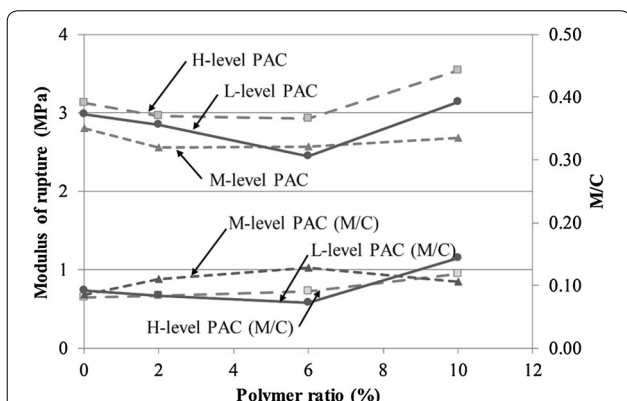


Fig. 18 Tensile strengths and tensile-to-compressive strength (M/C) ratios.

concrete samples had rather smaller moduli of rupture than the L-level aggregate concrete samples; i.e., the moduli of rupture of C-M-10 and C-M-0 were approximately 14.6 and 6.0% smaller than those of C-L-10 and C-L-0, respectively. This suggests that partial aggregate cleaning might cause a reduction in the tensile strength of PAC with recycled ballast aggregates.

4.3 Shrinkage Strain

The results of the shrinkage tests for the concrete samples are presented in Fig. 19. Overall, the shrinkage strain rapidly increased at the early curing stage, but after about 15–20 days, the change in shrinkage strain became insignificant.

The concrete samples with 2% polymer ratio exhibited a significant increase in shrinkage strain during a few hours immediately after the beginning of the strain measurement (Fig. 19). In contrast, early expansion, signified by positive strain values, was observed for the samples with higher polymer ratios. In particular, it

was the greatest in the samples with 10% polymer ratio (Fig. 19). The difference in early expansion in relation to the polymer ratio was possibly due to the following reasons: (1) re-emulsified polymer particles inhibited the reaction between cement and water (as discussed for the early compressive strength results), and consequently delayed the shrinkage. (2) At the same time, re-emulsified polymer particles might enlarge in volume to cause the expansion of concrete under the unconstrained condition (Ohama 1995).

The ultimate shrinkage strain of concrete gradually decreased as the polymer ratio increased; for example, C-H-6 and C-L-6 underwent more than 30% smaller peak strains compared with C-H-2 and C-L-2, respectively (Fig. 19). The reduction in the ultimate shrinkage strain with a higher polymer ratio was likely because continuous polymer films occupying micro-pores in the concrete hindered water evaporation (Su 1995; Persson 2001; Zhang and Kong 2014). Furthermore, it was possibly in part because re-emulsified polymer particles might enlarge in volume to offset the shrinkage.

With regard to the effect of the cleanness level of ballast aggregates, C-L-2 and C-L-6 underwent a smaller shrinkage strain than C-H-2 and C-H-6, respectively. This could be possibly because the fine particles attached to ballast aggregates filled the micro-pores of concrete and consequently reduced the shrinkage strain (Li and Yao 2001). However, the effect of the aggregate cleanness on the shrinkage strain of concrete was not as significant as that of the polymer ratio.

4.4 Freezing–Thawing Resistance

The results of the freezing–thawing resistance tests for the concrete samples are presented in Fig. 20. The test results are generally in accordance with the flexure test results. The freezing–thawing resistance of PAC with

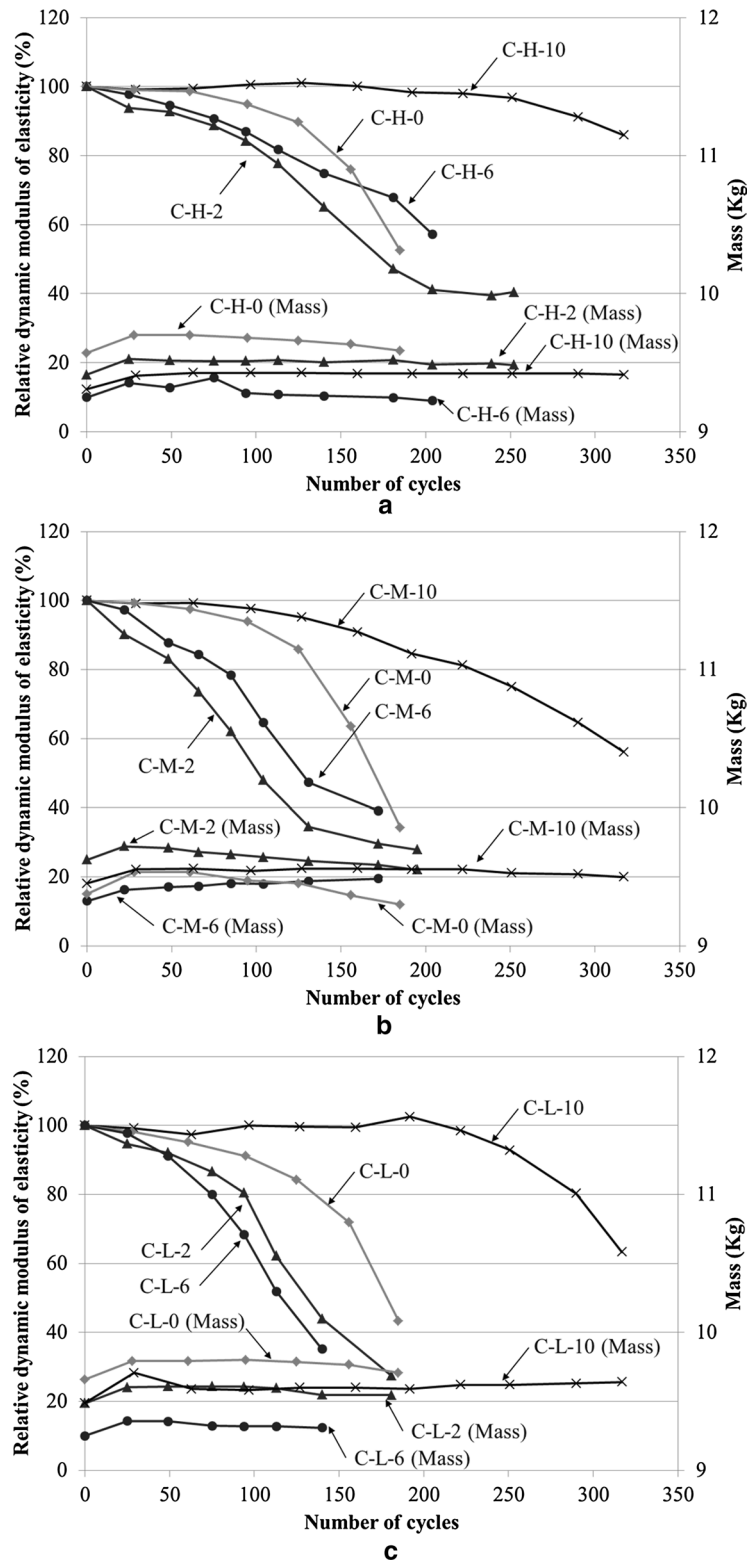


Fig. 20 Relative dynamic moduli of elasticity (RDMs) of concrete samples with **a** H-level, **b** M-level, and **c** L-level aggregates.

Table 6 Durability factors of the twelve concrete samples.

Polymer ratio (%)	Durability factor (%) determined by Eq. (2)		
	Cleanness level of ballast aggregates		
	H-level	M-level	L-level
0	32.4	21.1	26.8
2	28.4	16.6	20.5
6	38.9	20.7	19.6
10	88.1	62.5	77.6

recycled ballast aggregates was not notably enhanced by the addition of 2 or 6% polymer. However, the concretes with a polymer ratio of 10% (C-H-10, C-M-10, and C-L-10) exhibited substantially higher freezing–thawing resistance. Among the H-level aggregate concretes, C-H-2 firstly reached an RDM value below 60% near the 150th cycle, and C-H-0 and C-H-6 followed later in turn. However, the RDM of C-H-10 remained larger than 80% after 300 cycles (Fig. 20). Similarly, the durability factor of the samples with 10% polymer was roughly 2.7–3.0 times larger than those with no polymer, whereas the factor was not increased by the use of 2 or 6% polymer (Table 6).

At a given polymer ratio, the concretes with H-level aggregates showed higher freezing–thawing resistance than those with L- or M-level aggregates (Fig. 20). Moreover, the durability factor of concrete was the highest with H-level aggregates for every polymer ratio (Table 6). This was likely in part because polymer played a more pronounced role in the ITZs of H-level aggregates with fewer alien particles, which would have hindered the formation of polymer films.

The mass of each specimen did not change much in all samples throughout the freezing–thawing tests (Fig. 20); only small mortar parts peeled from the surfaces of the specimens. This implies that the degradation of the freezing–thawing resistance of PAC with recycled ballast aggregates originated mainly from interfacial failures between the aggregates and mortar. The freezing–thawing test results were clearly visualized in the specimen sections that were cut after the completion of testing (Figs. 21 and 22): (1) the concretes with 10% polymer displayed the least damage in the ITZs, regardless of the aggregate cleanness level (Figs. 21d and 22d). (2) The concretes with L-level aggregates (Fig. 22) experienced more extensive damage in the ITZs than those with H-level aggregates (Fig. 21).

Figures 23 and 24 show the magnified images of damaged ITZs in H- and L-level aggregate concretes,

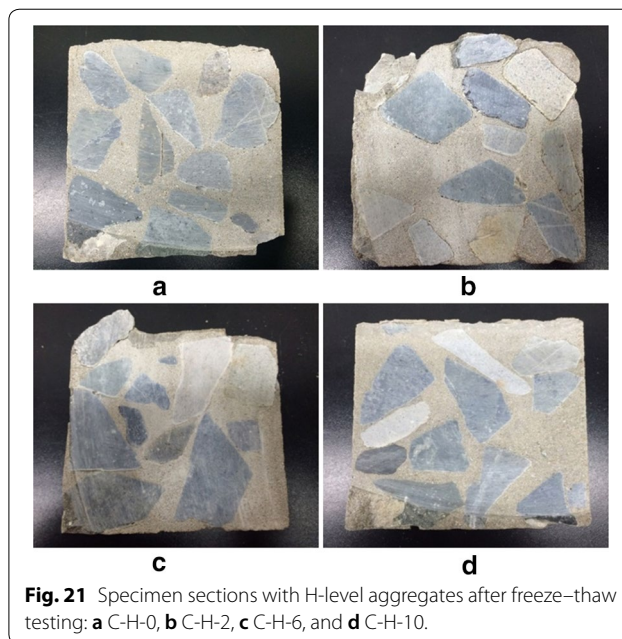


Fig. 21 Specimen sections with H-level aggregates after freeze–thaw testing: **a** C-H-0, **b** C-H-2, **c** C-H-6, and **d** C-H-10.

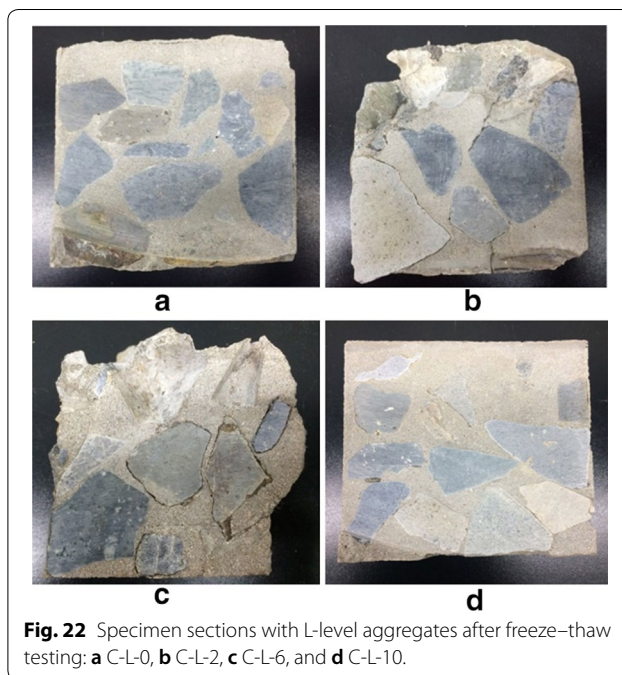


Fig. 22 Specimen sections with L-level aggregates after freeze–thaw testing: **a** C-L-0, **b** C-L-2, **c** C-L-6, and **d** C-L-10.

respectively, taken by an optical microscope with a magnification factor of 160 after the freeze–thaw tests. The concretes with low RDM and DM values clearly experienced severe crack damages in the ITZs; the crack width in C-L-2 and C-L-6 was approximately of the order of

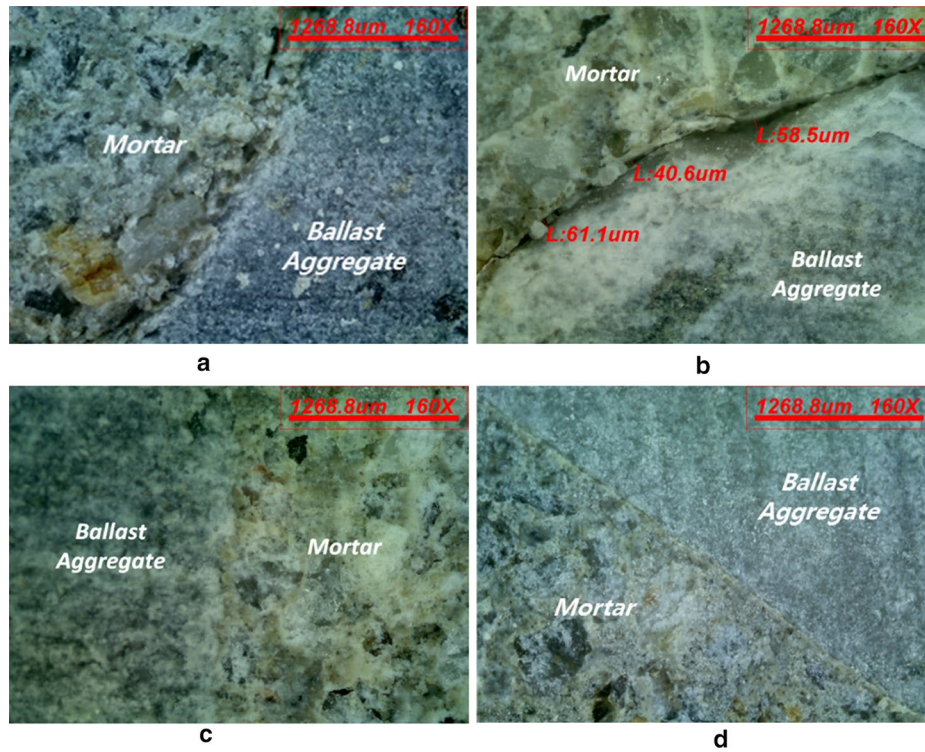


Fig. 23 Damaged ITZs with H-level aggregates after freeze–thaw testing: **a** C-H-0, **b** C-H-2, **c** C-H-6, and **d** C-H-10 [magnification factor: 160].

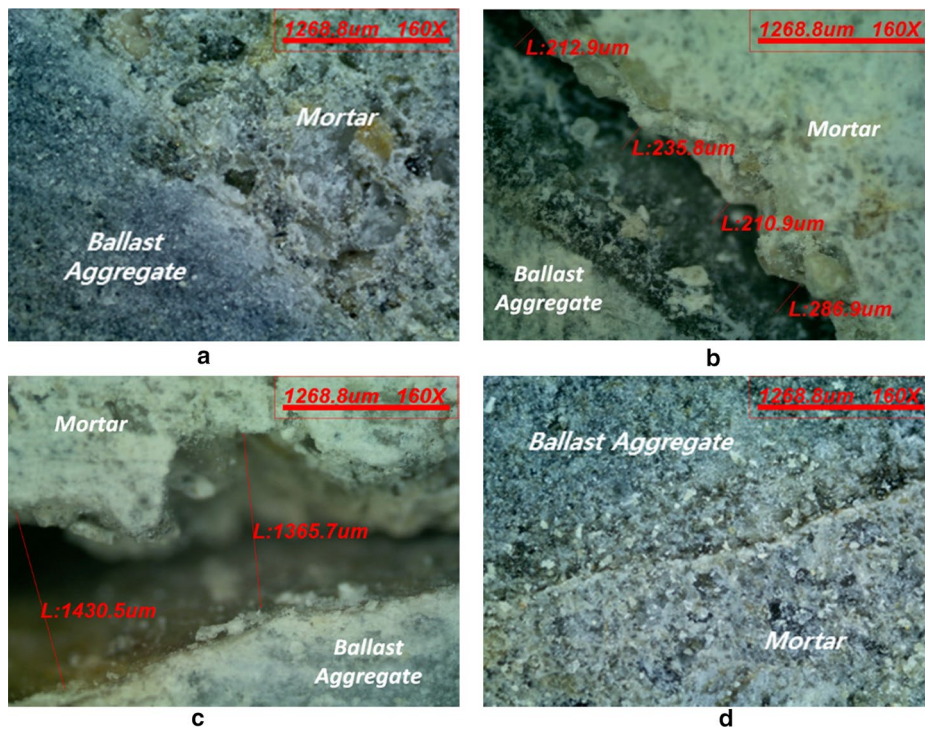


Fig. 24 Damaged ITZs with L-level aggregates after freeze–thaw testing: **a** C-L-0, **b** C-L-2, **c** C-L-6, and **d** C-L-10 [magnification factor: 160].

0.3–1.4 mm. In contrast, considerable damages were not found in the ITZs of the concretes with the highest RDM and DF values (e.g., C-H-10).

5 Conclusion

The experimental results obtained in this study led to the following findings and conclusions:

1. The 28-day compressive strength of both mortar and concrete produced from recycled ballast aggregates generally decreased as the polymer ratio increased. The increase in the polymer ratio also caused a reduction in the modulus of elasticity of concrete.
2. In contrast, the addition of redispersible polymer powder generally increased the tensile strength of the concrete. This was likely owing to the improvement of ITZs between the aggregates and mortar.
3. The ultimate shrinkage strain of the concrete decreased gradually as the polymer ratio increased. In the concrete samples with 2% polymer ratio, the shrinkage strain drastically increased during a few hours at the early curing stage. In contrast, early expansion was observed in the concretes with higher polymer ratios.
4. The freezing–thawing resistance of the concrete was significantly increased at a polymer ratio of 10%, whereas it was not notably enhanced by the use of 2 or 6% polymer. From the microscope images, it is evident that the degradation of freezing–thawing resistance originated mainly from the failure of the ITZs.
5. The concrete samples with H-level aggregates generally showed higher compressive strength, tensile strength, and freezing–thawing resistance than those with L- and M-level aggregates.
6. The shrinkage strain of the concrete generally decreased as the aggregates were cleaned to a lesser extent, but the effect of the aggregate cleanness was not as significant as that of the polymer ratio.
7. The setting and early strength development of the concrete was delayed as the amount of polymer increased. This delay likely occurred because the polymer particles produced films around the cement grains to inhibit the reaction between cement and water. Further microstructural analyses are underway to investigate the effect of the polymer on the microstructure and strength development of CSA cement systems at short-term as well as long-term curing periods.

Authors' contributions

SL conducted experiments, analyzed experimental results, and prepared the first full version of the manuscript and the revised version; SYJ contributed to improving the manuscript by technical guidance, comments, and revision; CYK, EJA, SPK, and SG contributed to preparation and testing of raw materials,

production of test specimens, and performance of experiments; and MS planned the research, acquired the research fund, supervised the overall process of the research and paper writing, and was in charge of the revision of the manuscript. All authors read and approved the manuscript.

Author details

¹ School of Urban and Environmental Engineering, Ulsan National Institute of Science and Technology (UNIST), 50 UNIST-gil, Ulsan 44919, Republic of Korea. ² Korea National University of Transportation, Uiwang, Gyeonggi-do 16106, Republic of Korea.

Acknowledgements

This research was supported by a Grant (15RTRP-B065581-03) from the Railway Technology Research Program of the Ministry of Land, Infrastructure and Transport, as well as a Grant (No. 18SCIP-B103706-04) from the Construction Technology Research Program funded by the Ministry of Land, Infrastructure and Transport of the Republic of Korea.

Competing interests

The authors declare that they have no competing interests.

Publisher's Note

Springer Nature remains neutral with regard to jurisdictional claims in published maps and institutional affiliations.

Received: 10 November 2017 Accepted: 23 August 2018

Published online: 20 November 2018

References

- ACI Committee 304. (2000). *Guide for measuring, mixing, transporting, and placing concrete*. Farmington Hills, MI: American Concrete Institute.
- ACI Committee 318. (2014). *Building code requirements for structural concrete (ACI 318-14) and commentary*. Farmington Hills, MI: American Concrete Institute.
- Aggarwal, L. K., Thapliyal, P. C., & Karade, S. R. (2007). Properties of polymer-modified mortars using epoxy and acrylic emulsions. *Construction and Building Materials*, 21(2), 379–383.
- ASTM C109. (2016). *Standard test method for compressive strength of hydraulic cement mortars (ASTM C109)*. West Conshohochon, PA: American Society for Testing and Materials.
- ASTM C192. (2016). *Standard practice for making and curing concrete test specimens in the laboratory (ASTM C192)*. West Conshohochon, PA: American Society for Testing and Materials.
- ASTM C39. (2016). *Standard test method for compressive strength of cylindrical concrete specimens (ASTM C39)*. West Conshohochon, PA: American Society for Testing and Materials.
- ASTM C469. (2014). *Standard test method for static modulus of elasticity and Poisson's ratio of concrete in compression (ASTM C469)*. West Conshohochon, PA: American Society for Testing and Materials.
- ASTM C666. (2016). *Standard test method for resistance of concrete to rapid freezing and thawing (ASTM C666)*. West Conshohochon, PA: American Society for Testing and Materials.
- ASTM C78. (2016). *Standard test method for flexural strength of concrete (using simple beam with third-point loading) (ASTM C78)*. West Conshohochon, PA: American Society for Testing and Materials.
- Bezin, Y., Farrington, D., Penny, C., Temple, B., & Iwnicki, S. (2010). The dynamic response of slab track constructions and their benefit with respect to conventional ballasted track. *Vehicle System Dynamics*, 48, 175–193.
- Choi, H., Choi, H., Lim, M., Inoue, M., Kitagaki, R., & Noguchi, T. (2016a). Evaluation on the mechanical performance of low-quality recycled aggregate through interface enhancement between cement matrix and coarse aggregate by surface modification technology. *International Journal of Concrete Structures and Materials*, 10(1), 87–97.
- Choi, J. Y., Joo, M. K., & Lho, B. C. (2016b). Effects of silica fume content and polymer-binder ratio on properties of ultrarapid-hardening polymer-modified mortars. *International Journal of Concrete Structures and Materials*, 10(2), 249–256.

- Galvín, P., Romero, A., & Domínguez, J. (2010). Vibrations induced by HST passage on ballast and non-ballast tracks. *Soil Dynamics and Earthquake Engineering*, 30(9), 862–873.
- Higuchi, Y., Harada, Y., Sato, T., Nakagawa, K., Kawaguchi, I., & Kasahara, Y. (1978). U.S. Patent No. 4,084,981. Washington, DC: U.S. Patent and Trademark Office.
- Jang, S. Y., Lee, I. W., & Kang, Y. S. (2013). Track system technology for future advanced railway construction. *Journal of the Korean Society of Civil Engineers*, 61(9), 41–51.
- Jun, L., Chang-wei, X., Xiao-yan, Z., & Ling-ling, W. (2003). Modification of high performances of polymer cement concrete. *Journal of Wuhan University of Technology-Mater. Sci.*, 18(1), 61–64.
- Kang, T. H. K., Kim, W., Kwak, Y. K., & Hong, S. G. (2014). Flexural testing of reinforced concrete beams with recycled concrete aggregates. *ACI Structural Journal*, 111(3), 607–616.
- Kardon, J. B. (1997). Polymer-modified concrete: Review. *Journal of Materials in Civil Engineering*, 9(2), 85–92.
- Kim, J. H., & Robertson, R. E. (1998). Effects of polyvinyl alcohol on aggregate-paste bond strength and the interfacial transition zone. *Advanced Cement Based Materials*, 8(2), 66–76.
- Kim, K., Shin, M., & Cha, S. (2013). Combined effects of recycled aggregate and fly ash towards concrete sustainability. *Construction and Building Materials*, 48, 499–507.
- Korean Railroad Research Institute (2014) Annual report on development of quick hardening technology for ballasted track of high-speed railway. Korea.
- Korean Railroad Research Institute (2015) Annual report on development of quick hardening technology for ballasted track of high-speed railway. Korea.
- Korean Standards Association. (2014a). *Standard test method for making and curing concrete specimens (KS F 2403)* (p. 2014). Seoul, Korea: Korean Agency for Technology and Standards.
- Korean Standards Association. (2014b). *Recycled aggregate for concrete (KS F 2573)* (p. 2014). Seoul, Korea: Korean agency for technology and standards.
- Lee, I. W. (2010). Improvement of dry-blasting efficiency for ballast used as aggregate of paved track. *Journal of Korean Society for Railway*, 13(1), 78–83.
- Lee, I. H., Kim, S. I., Kim, Y. J., Kim, D. G., Kim, T. H., & Jeong, C. S. (2015). A Study on the development of waterless gravel cleaning system for high-speed train ballast gravel recycle. *Proceedings of the Korean Society for Railway Conference*, 453–458.
- Lee, I. W., Pyo, S., & Jung, Y. H. (2016). Development of quick-hardening infilling materials for composite railroad tracks to strengthen existing ballasted track. *Composites Part B Engineering*, 92, 37–45.
- Li, J., & Yao, Y. (2001). A study on creep and drying shrinkage of high performance concrete. *Cement and Concrete Research*, 31(8), 1203–1206.
- Liu, S., Kong, Y., Wan, T., & Zhao, G. (2018). Effects of thermal-cooling cycling curing on the mechanical properties of EVA-modified concrete. *Construction and Building Materials*, 165, 443–450.
- McNeil, K., & Kang, T. H. K. (2013). Recycled concrete aggregates: a review. *International Journal of Concrete Structures and Materials*, 7(1), 61–69.
- Miura, S., Takai, H., Uchida, M., & Fukada, Y. (1998). The mechanism of railway tracks. *Japan Railway & Transport Review*, 2, 38–45.
- Muñoz, J. F., Gullerud, K. J., Cramer, S. M., Tejedor, M. I., & Anderson, M. A. (2005). Effects of coarse aggregate coatings on concrete performance. *Journal of Materials in Civil Engineering*, 22(1), 96–103.
- Murao, K., & Aihara, H. (2005). Development of low-maintenance tracks. *JR EAST Technical Review*, 6, 16–22.
- Najjar, M. F., Soliman, A. M., & Nehdi, M. L. (2014). Critical overview of two-stage concrete: Properties and applications. *Construction and Building Materials*, 62, 47–58.
- Norvell, J. K., Stewart, J. G., Juenger, M. C., & Fowler, D. W. (2007). Influence of clays and clay-sized particles on concrete performance. *Journal of Materials in Civil Engineering*, 19(12), 1053–1059.
- Ohama, Y. (1995). *Handbook of polymer-modified concrete and mortars, properties and process technology*. Park Ridge, NJ, USA: Noyes Publications.
- Paixão, A. M., Fortunato, E. C., & Antunes, M. L. (2009). Emerging trends for high-speed rail track superstructures—Ballastless track as an alternative to the ballasted track. In: *Bearing Capacity of Roads, Railways and Airfields—Proceedings of the 8th International Conference on the Bearing Capacity of Roads, Railways and Airfields*, 2, 1231–1241.
- Persson, B. (2001). A comparison between mechanical propel-ties of self-compacting concrete and the corresponding properties of normal concrete. *Cement and Concrete Research*, 31(2), 193–198.
- Qudoos, A., Kim, H. G., & Ryou, J. S. (2018). Influence of the surface roughness of crushed natural aggregates on the microhardness of the interfacial transition zone of concrete with mineral admixtures and polymer latex. *Construction and Building Materials*, 168, 946–957.
- Rossignolo, J. A., & Agnesini, M. V. C. (2004). Durability of polymer-modified lightweight aggregate concrete. *Cement & Concrete Composites*, 26(4), 375–380.
- Sakai, E., & Sugita, J. (1995). Composite mechanism of polymer modified cement. *Cement and Concrete Research*, 25(1), 127–135.
- Shaker, F., El-Dieb, A. S., & Reda, M. M. (1997). Durability of Styrene-Butadiene latex modified concrete. *Cement and Concrete Research*, 27(5), 711–720.
- Su, Z. (1995). Microstructure of polymer cement concrete, *PhD thesis*, Material Sciences Group, Delft University of Technology, Delft, Netherlands.
- Su, Z., Bijen, J. M. J. M., & Larbi, J. A. (1991). Influence of polymer modification on the hydration of portland cement. *Cement and Concrete Research*, 21(4), 535–544.
- Wang, R., Li, X. G., & Wang, P. M. (2006). Influence of polymer on cement hydration in SBR-modified cement pastes. *Cement and Concrete Research*, 36(9), 1744–1751.
- Wang, M., Wang, R., Yao, H., Farhan, S., Zheng, S., Wang, Z., et al. (2016). Research on the mechanism of polymer latex modified cement. *Construction and Building Materials*, 111, 710–718.
- Yang, H. G., & Joo, J. W. (2011). Measurement of thermal expansion coefficient using strain gage, *Proceedings of the Korean Society of Mechanical Engineers Conference*, 404–409.
- Yoo, W. H., Lee, I. H., Jang, S. Y., & Jung, Y. S. (2016). Development of durable-performance improvement infilling for ballasted track of high-speed railway. *Proceedings of the Korean Society for Railway Conference*, 287–292.
- Zhang, Y., & Kong, X. (2014). Influences of superplasticizer, polymer latexes and asphalt emulsions on the pore structure and impermeability of hardened cementitious materials. *Construction and Building Materials*, 53, 392–402.